Asian Journal of Chemistry; Vol. 35, No. 11 (2023), 2683-2688

ASIAN JOURNAL OF CHEMISTRY

https://doi.org/10.14233/ajchem.2023.28421

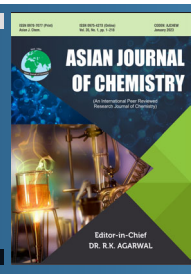

Electrochemical Synthesis and Characterization of Poly(*p*-Toluidine-*co*-*o*-aminophenol) Copolymers: Influence of Monomer Ratio

M. SHANTHAMANI[1,*] and K. KARTHIK[2]

[1]P.G. & Research Department of Chemistry, Government Arts College, Coimbatore-641018, India
[2]Department of Chemistry, School of Foundational Sciences, Kumaraguru College of Technology, Coimbatore-641049, India

*Corresponding author: E-mail: shanthache@gmail.com

Received: 29 July 2023; *Accepted*: 4 September 2023; *Published online*: 31 October 2023; AJC-21423

Conducting polymers, particularly poly(*p*-toluidine) (PPT) and its copolymer films with poly(*o*-aminophenol) [poly(PT-*co*-OAP)], have gained significant attention due to their diverse applications in batteries, electronic devices, sensors, *etc*. The copolymers were prepared using electrochemical method using cyclic voltammetry on an indium tin oxide (ITO) coated glass plate immersed in a solution of 1 M HCl. The influence of the monomer ratio on the resulting copolymerization and electrochemical behaviour was also investigated. Additionally, a possible mechanism for Poly(PT-*co*-OAP) formation in an acidic medium is also deduced. The synthesized copolymers were thoroughly characterized using IR, UV-Vis, PXRD, SEM and conductivity analysis.

Keywords: Copolymerization, Cyclic voltammetry, Electrochemical behaviour, Poly(*p*-toluidine), Poly(*o*-aminophenol).

INTRODUCTION

Conducting polymers have garnered extensive attention in various emerging fields due to their versatile applications, including batteries [1-3], electronic devices, catalysts, sensors, capacitors, electromagnetic radiation shielding, gas separation membranes, antistatic coatings, nonlinear optics and electrochromic devices [4-7]. Prominent examples of common conducting polymers include polyacetylene (PA), polyaniline (PANI), polypyrrole (PPy), polythiophene (PTH), poly(*p*-phenylene) (PPP), poly(phenylenevinylene) (PPV) and polyfuran (PF). Notably, polyaniline (PANI) exhibits spontaneous protonation or oxidation in aqueous acidic solutions, making it particularly beneficial for battery capacity recovery [8,9]. Poly(aniline-*co*-*o*-aminophenol) has also demonstrated good electrochemical properties at a pH of approximately 10.6, accompanied by relatively high conductivity [10].

Extensive studies are reported on the synthesis and electrochemistry of polyanilines and polyaniline-substituted alkyl ring polyanilines [11,12]. Polymers can be created through chemical and/or electrochemical polymerization processes, with many redox polymers being chemically synthesized. Electrochemically active groups can be incorporated into the polymer chain's internal structure, introduced as pendant groups (functionalized polymers) included during polymerization's polymer phase or fixed into the polymer network in post-coating functionalization steps. The preparation of copolymers using aniline as the parent monomer and alkyl ring-substituted anilines as comonomers has been reported [13]. Electrochemical synthesis *via* cyclic voltammetry has enabled the preparation of poly(alkyl anilines), which were found to be modified with alkyl substitution during the polymerization process.

In present study, the growth behaviour of copolymers based on *p*-toluidine (PT) and *o*-aminophenol (OAP) was monitored under different conditions. The copolymers were synthesized through the oxidative polymerization in an acidic medium, resulting in hydrochloric acid doped poly(*ortho*-aminophenol-*co*-*p*-toluidine), a conjugated semiconducting copolymer. To characterize the synthesized polymers comprehensively, we conducted UV-Vis, IR, SEM, PXRD and conductivity studies.

EXPERIMENTAL

o-Aminophenol (Morli, Mumbai), *p*-toluidine (Reachem, Chennai, India) and potassium peroxodisulphate (PDS) were used without further purification. Solvents used included hydrochloric acid, nitric acid, sulphuric acid (Fischer, India),

chloroform, methanol, ethanol (Reachem, Chennai), dimethyl formamide (DMF) and dimethyl sulphoxide (DMSO).

Synthesis of homopolymer: The homopolymer of *p*-toluidine (PT) was chemically synthesized using potassium peroxodisulphate (PDS) as an oxidant. To prepare 100 mM PPT, 4.28 mL of PT was dissolved in a pre-cooled solution of 400 mL of 1 M HCl. Next, a pre-cooled solution of 100 mL PDS (200 mM) containing 5.4 g of PDS in 1 M HCl was slowly added dropwise to the PT monomer solution with constant stirring for 2 h. The resulting solution was further stirred for approximately 1 h in a freezing mixture. During this process, a green-coloured precipitate formed, which was poly(*p*-toluidine) doped with HCl (acid-doped PPT).

To isolate the acid doped PPT, the green precipitate was filtered through a sintered glass crucible and continuously washed with 1 M HCl. Finally, the acid doped PPT was dried under an air oven at 80 ºC for 1 h. A similar procedure was followed for the synthesis of poly(*o*-aminophenol) (POAP) and the copolymers.

Cyclic voltammetry measurements: The cyclic voltammetry (CV) measurements were performed using a Shimadzu 2101-PC instrument on polymer films deposited on an optically transparent indium tin oxide (ITO) glass electrode. A standard 10 mm cuvette was used as the supporting electrolyte solution. For *in situ* resistance measurements, a band-gap gold electrode, as described elsewhere, was used as the working electrode. A gold sheet served as the counter electrode, while an Hg/HgCl electrode was used as the reference electrode. The CV voltammograms were recorded over a potential range of -0.2 to +1.2 V at a scan rate of 50 mV/s. The measurements were carried out at room temperature and the voltammograms were recorded in the negative potentials to assess reversibility.

UV-visible studies: Electronic absorption spectra of the doped polymers were recorded using a Lab India UV/VIS spectrometer. The spectra were obtained in DMF and DMSO solvents, covering a wavelength range of 190-800 nm. The measurements were conducted at room temperature.

FT-IR studies: To characterize further the prepared polymers, Fourier-transform infrared (FTIR) spectra were obtained using a Brucker-Alpha model instrument. The spectra were recorded in the region of 4000-400 cm^{-1}, allowing for the analysis of the functional groups and chemical bonds present in the polymers.

SEM studies: The surface morphology of the copolymer film was studied using a HITACHI 347 SEI scanning electron microscope (SEM). This analysis provided visual insights into the structural features and surface topography of the copolymer film.

XRD studies: To assess the crystalline structure of the polymer samples, the X-ray diffraction (XRD) patterns were obtained using a SAIFXRI130702A diffractometer equipped with a computer interface system. The XRD analysis allowed the observation of the characteristic diffraction peaks that indicate the presence of crystalline regions in the polymer samples.

RESULTS AND DISCUSSION

Electrochemical behaviour studies: During the electropolymerization process of *p*-toluidine (PT), *o*-aminophenol (OAP) and mixtures of PT and OAP with different feed ratios in 1 M HCl electrolyte, cyclic voltammograms (CVs) were recorded on an indium tin oxide (ITO) electrode surface. The potential was cycled between -0.2 V and 1.2 V *versus* a mercury/mercury chloride (Hg/HgCl) reference electrode at a scan rate of 50 mV/s. The total concentration of both monomers was maintained at 100 mM in all cases.

For the polymerization of PT with various molar feed ratios of OAP (0.1, 0.5 and 0.9), the cyclic voltammograms were continuously recorded for 25 cycles. The resulting CVs showed distinct peak characteristics for each scenario. When using 100 mM of PT alone, three anodic peaks (E_{pa}(I) 0.005 V, E_{pa}(II) 0.225 V and E_{pa}(III) 0.302 V) and three cathodic peaks (E_{pc}(I) 0.025 V, E_{pc}(II) 0.271 V and E_{pc}(III) 0.455 V) were observed (Fig. 1). Conversely, the CV of 100 mM OAP exhibited two oxidation peaks at 0.03 V and 0.147 V and two reduction peaks at 0.186 V and 0.489 V (Fig. 2).

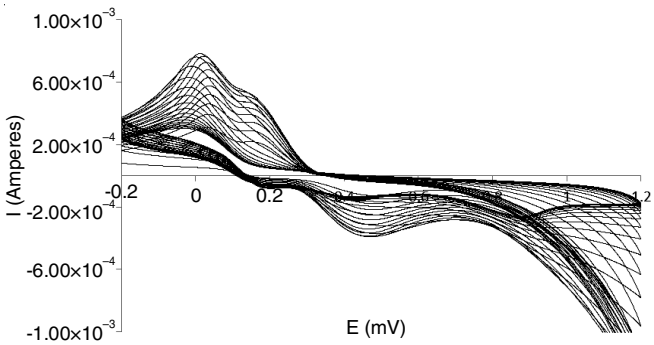

Fig. 1. Cyclic voltammograms of poly *p*-toludine films deposited for 25 cycles, E_c/E_a = -0.2/1.2 V, scan rate = 50 mV/s, PT = 100 mM

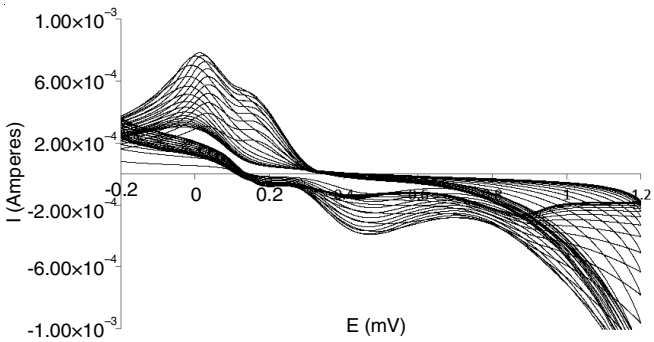

Fig. 2. Cyclic voltammograms of poly *o*-aminophenol films deposited for 25 cycles, E_c/E_a = -0.2/1.2 V, scan rate = 50 mV/s, OAP = 100 mM

For the equimolar feed ratio of PT with OAP (1:1), the CV displayed three anodic peaks at 0.028 V, 0.106 V and 0.194 V and three cathodic peaks at 0.039 V, 0.155 V and 0.416 V (Fig. 3). On the other hand, when the feed ratio of PT with OAP was 0.9:0.1, the CV exhibited three oxidation peaks at 0.014 V, 0.102 V and 0.174 V and three reduction peaks at 0.005 V, 0.146 V and 0.426 V (Fig. 4). Similarly, the cathodic peaks appeared for the feed ratio of 0.1:0.9 at 0.141 V and 0.482 V, along with two anodic peaks at 0.116 V and 0.482 V (Fig. 5). Interestingly, a pair of oxidation peaks within the range of 0.116 V and 0.194 V was identified to be associated with the growth behaviour of the copolymer. These peaks were

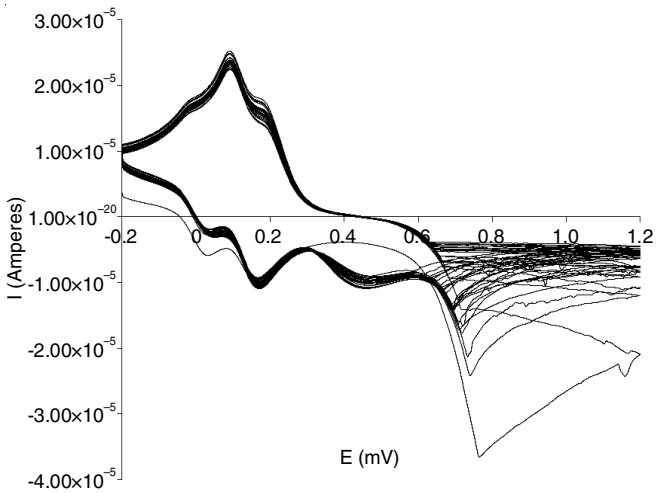

Fig. 3. Cyclic voltammograms of poly(PT-*co*-OAP) films deposited for 25 cycles, E_c/E_a = -0.2/1.2 V, scan rate = 50 mV/s, PT = 50 mM; OAP = 50 mM

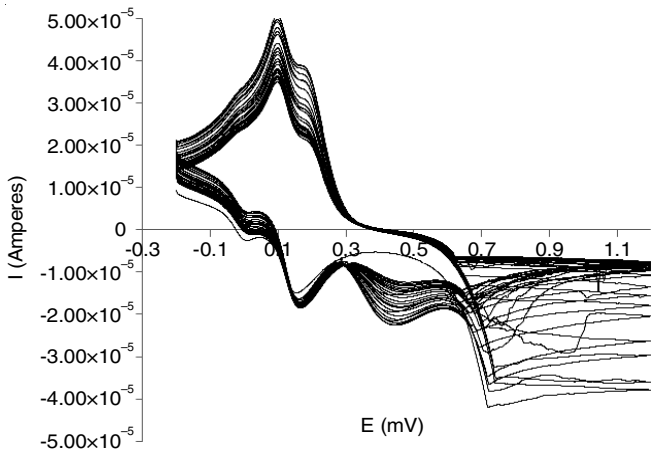

Fig. 4. Cyclic voltammograms of poly(PT-*co*-OAP) films deposited for 25 cycles, E_c/E_a = -0.2/1.2 V, scan rate = 50 mV/s, PT = 90 mM; OAP = 10 mM

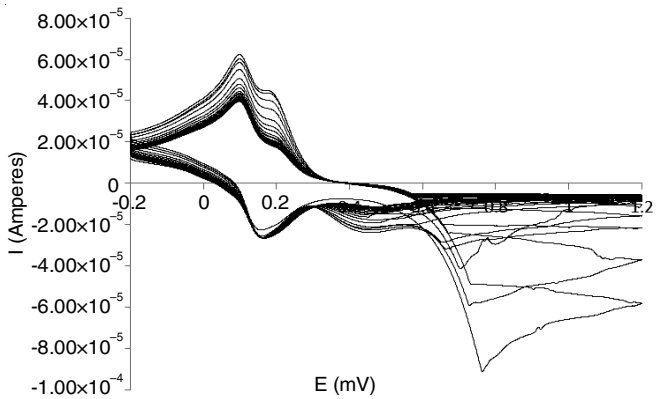

Fig. 5. Cyclic voltammograms of poly(PT-*co*-OAP) films deposited for 25 cycles, E_c/E_a = -0.2/1.2 V, scan rate = 50 mV/s, PT = 10 mM; OAP = 90 mM

different from the peaks obtained for both individual monomers, indicating the distinct behaviour of the copolymer.

The observed shifts in the peaks and the differences in their tendencies during the PT polymerization and copolymerization with OAP suggest that the concentration of OAP in the feed influences the overall oxidation state of the resulting copolymer. Based on this observation, a possible mechanism for the formation of the copolymer poly(PT-*co*-OAP) is deduced (**Scheme-I**).

UV-Visible studies: For the UV-Vis analysis, the doped polymer samples were dispersed in DMSO and their spectra were obtained. The UV-Vis spectra (Fig. 6) of the doped polymers showed typical behaviour characterized by two absorption bands. The first absorption band (λ_{max}(I) 315 nm) corresponds to the π-π* transition, which is indicative of the presence of a conjugated system in the benzenoid ring. This band indicates the presence of a well-defined conjugated structure in the polymer, which is a characteristic feature of conducting polymers. The second absorption band (λ_{max}(II) 480 nm) is attributed to the n-π* transition, which is a π*-polaron transition. This transition indicates the presence of an intermediate state between the leucomeraldine form, which contains benzenoid rings and the emeraldine form in the main chain of the polymer. This transition involves the movement of charges and represents a key step in the redox process of the conducting polymer.

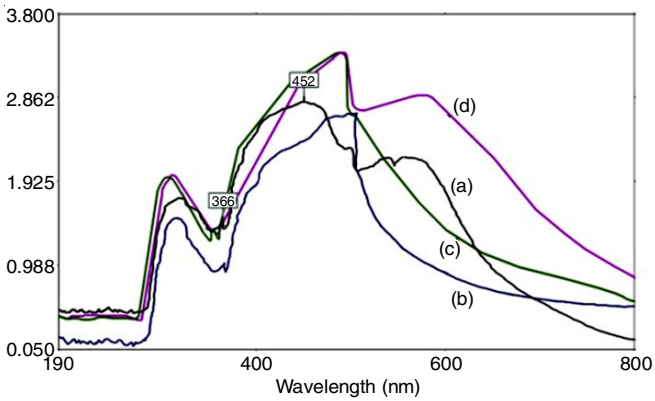

Fig. 6. UV-visible spectrum of poly(PT-*co*-OAP) (a) 100 mM PT, (b) 100 mM OAP, (c) 30:70, (d) 70:30

Additionally, the third absorption band (λ_{max}(III) 582 nm) is assigned to another π*-polaron transition. In this case, the transition corresponds to the formation of molecular excitons resulting from charge transfer into the quinoid ring from neighbouring benzenoid rings. This further confirms the presence of a well-defined conjugated system and the charge transfer characteristics of the doped polymer.

FTIR spectrum: In this study, the FTIR spectrum was recorded for three samples: PPT (homopolymer of *p*-toluidine), POAP (homopolymer of *o*-aminophenol) and the copolymer poly(OA*P*-*co*-PT). The FTIR spectra were obtained using KBr pellets in the range of 4000-400 cm^{-1} (Fig. 7). Peaks around 3266 cm^{-1} are attributed to the NH stretching vibrations, indicating the presence of -NH groups in both monomer units (OAP and PT). The intensity of these peaks may vary in POAP and PPT, suggesting differences in the local environment or interactions involving NH groups. Peaks around 3620 cm^{-1} are assigned to -OH stretching vibrations in POAP. This indicates the presence of hydroxyl groups in the *o*-aminophenol monomer. A peak around 3060 cm^{-1} is the characteristic of C-H stretching

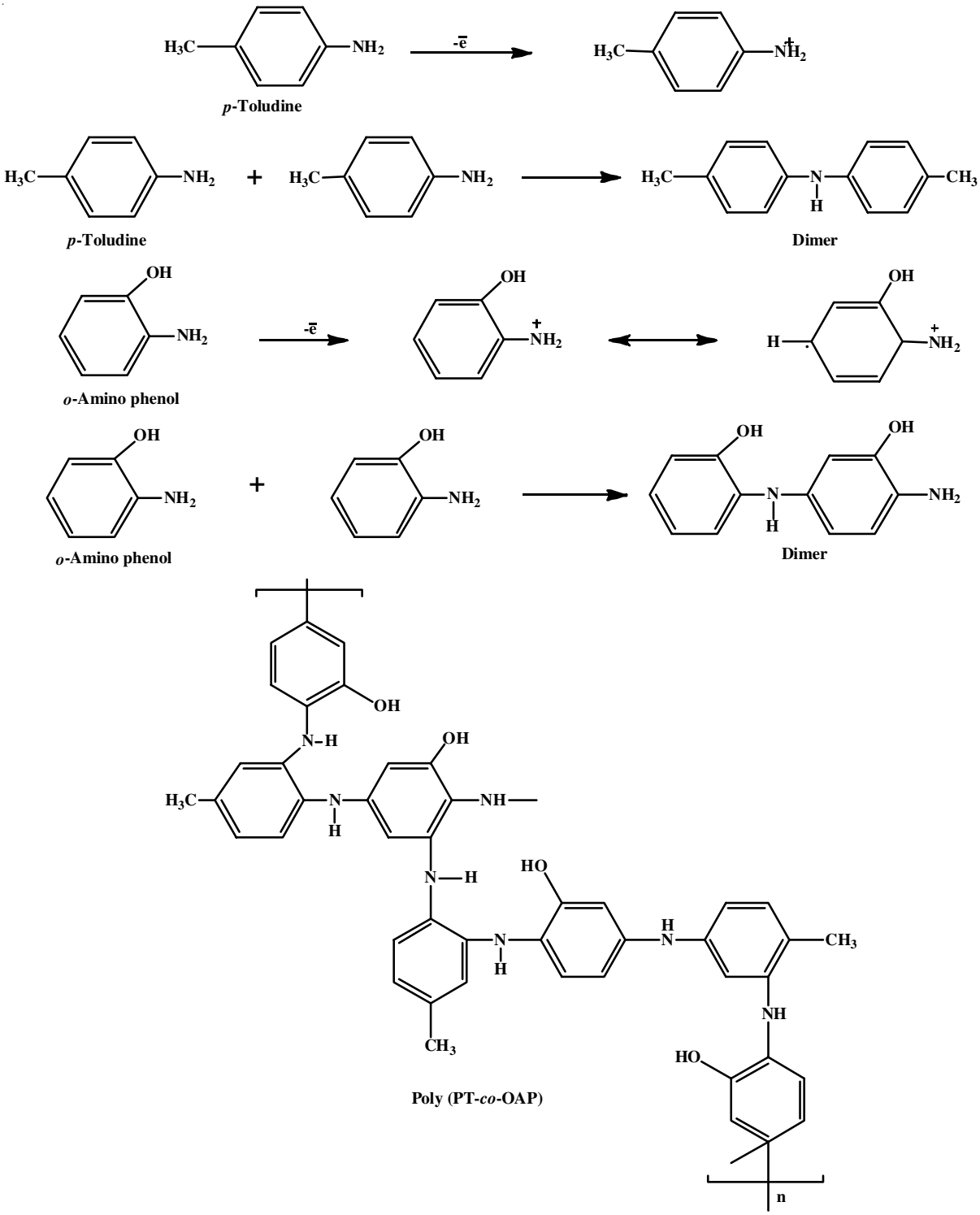

Scheme-I: Mechanism for the copolymerization of poly(PT-*co*-OAP)

vibrations in the aromatic ring of the copolymer sample, whereas peak at 1416 cm^{-1} corresponds to C-N stretching indicating the presence of C-N bonds in the copolymer. This further supports the formation of poly(OA*P*-*co*-PT) copolymer, indicating the incorporation of OAP units into the PT backbone. A peak at 766 cm^{-1} can be attributed to C-C stretching vibrations, indicating the presence of carbon-carbon bonds in the copolymer whereas the peak at 956 cm^{-1} corresponds to C-O stretching vibrations of the aromatic ring in the copolymer sample. Moreover, bands in the range of 3267, 1575 and 3612 cm^{-1} correspond to the N-H stretching, N-H bending and NH_2 groups, respectively. The presence of these bands in the copolymer structure confirms that the copolymer forms through the participation of the NH_2 group from the PT monomer and indicates the incorporation of OAP units into the PT backbone.

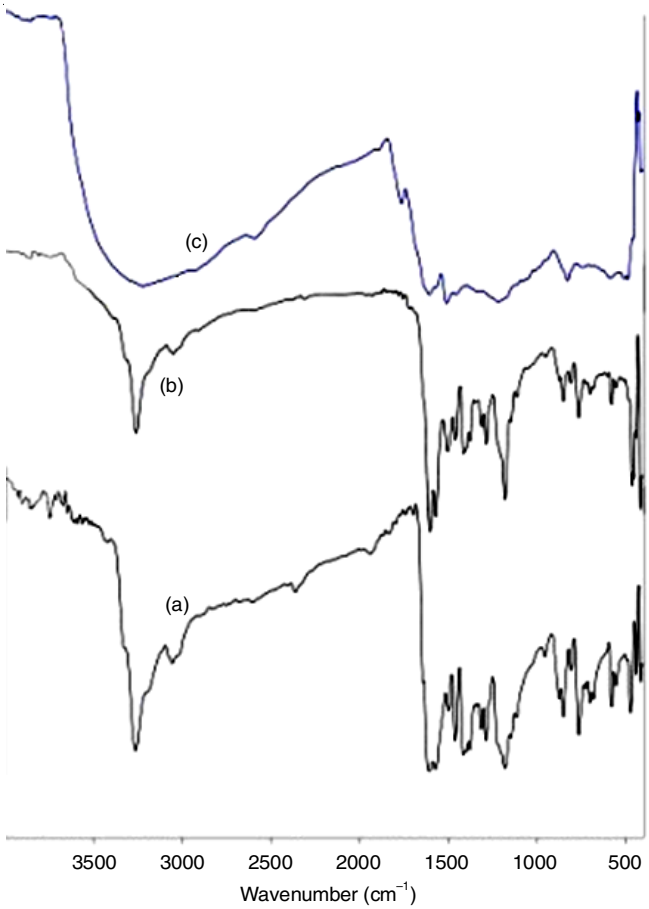

Fig. 7. FTIR spectra of polymers (a) POAP, (b) OAP:PT (70:30), (c) OAP:PT (30:70)

Scanning electron microscopy (SEM) and X-ray diffraction (XRD): The surface morphology of the homopolymer of *p*-toluidine (PPT) shows a crystalline structure with pores. This indicates that the PPT polymer has a well-defined and ordered arrangement of polymer chains, resulting in a relatively smooth and porous surface. The surface morphology of the homopolymer of *o*-aminophenol (POAP) appears spongy with agglomerated particles (Fig. 8). This suggests that the POAP polymer has a more irregular and less organized structure compared to PPT. The presence of agglomerated particles indicates some level of clustering or aggregation of polymer chains. The surface morphology of the copolymer of *p*-toluidine and *o*-aminophenol (PT-*co*-OAP) exhibits a porous and spongy-like structure with relatively agglomerated particles (Fig. 8). This suggests that the copolymer has a unique morphology combining characteristics of both PPT and POAP. The presence of both porous and spongy features indicates the incorporation of OAP units into the PT backbone, resulting in a different surface structure compared to the individual homopolymers.

The X-ray diffraction profile of PPT indicates a crystalline nature (Fig. 9). This means that PPT has a highly ordered and regular arrangement of polymer chains, resulting in distinct diffraction peaks in the XRD pattern. The X-ray diffraction profile of POAP shows an amorphous nature (Fig. 9). This suggests that POAP lacks long-range order in its polymer chain arrangement, resulting in a diffuse XRD pattern without distinct peaks. The X-ray diffraction profile of the copolymer indicates a more amorphous nature compared to PPT. This indicates that the incorporation of OAP units into the PT backbone reduces the overall crystallinity of the copolymer. The copolymer exhibits a less ordered arrangement of polymer chains compared to PPT, which aligns with the spongy-like surface morphology observed.

Conclusion

The cyclic voltammetry was used to deposit adherent polymeric films on an ITO plate from a mixture of *p*-toluidine

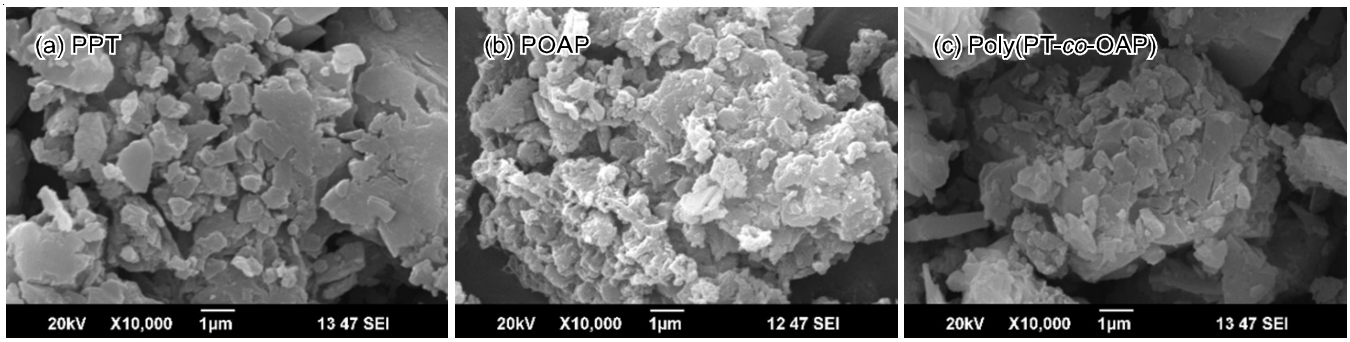

Fig. 8. SEM micrographs (a) PPT, (b) POAP, (c) poly(PT-*co*-OAP)

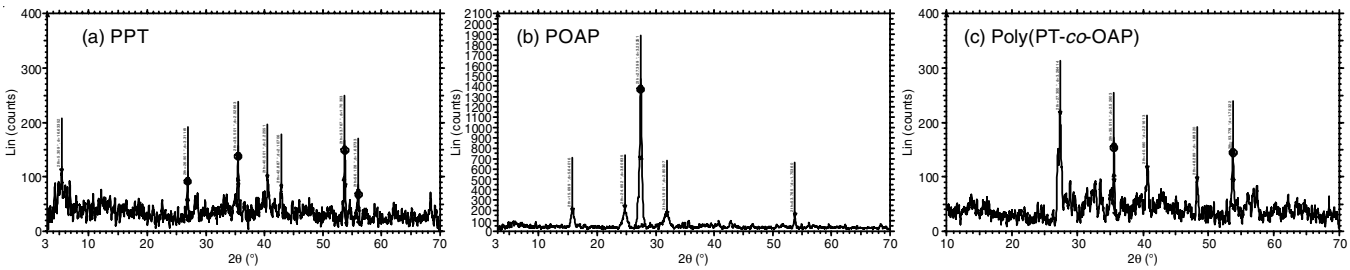

Fig. 9. X-ray diffraction of polymers (a) PPT, (b) POAP, (c) poly(PT-*co*- OAP)

(PT) and *o*-aminophenol (OAP) in a solution of 1 M HCl. The CV results showed distinct variations in the peak potentials of the redox processes for the copolymer poly(PT-*co*-OAP) compared to the individual homo polymers (PPT and POAP). This confirms the successful formation of the copolymer and justifies the use of both monomers in the electro-polymerization process. The electrical conductivity of the copolymer poly(PT-*co*-OAP) was measured and found to be 3.982×10^{-3} S cm^{-1}. In comparison, the POAP film had higher conductivity with a value of 5.445×10^{-3} S cm^{-1}. This suggests that the individual POAP monomer exhibits higher conductivity and stability compared to the copolymer. The electroactivity of PPT, POAP and poly(PT-*co*-OAP) was evaluated under different acidic conditions, revealing the protonation and deprotonating equilibrium associated with the oxidation and reduction of the copolymers. This information is important for understanding the electrochemical behaviour and potential applications of the synthesized copolymer. The surface morphology studies using scanning electron microscopy (SEM) and X-ray diffraction (XRD) revealed that PPT possesses a crystalline structure with pores. However, the copolymer poly(PT-*co*-OAP) showed a more amorphous structure with reduced crystallinity as it was polymerized with the comonomer OAP. The distinct differences in surface morphology and crystallinity indicate the successful incorporation of OAP units into the PPT backbone during copolymerization. The UV-Visible spectra of poly(PT-*co*-OAP) showed variations in the peak positions of the π-π* transitions of the benzenoid ring when compared to the spectra of PPT and POAP. These variations in peak positions suggest changes in the electronic structure and bonding in the copolymer compared to the individual homopolymers. The FTIR spectra provided information on the vibrational bands of the aromatic ring, including -NH stretching, OH stretching, C-H stretching and C-O stretching for PPT, POAP and the copolymers. Variations in the intensities and positions of these bands were observed, indicating differences in the molecular structure and functional groups between the three polymeric materials.

CONFLICT OF INTEREST

The authors declare that there is no conflict of interests regarding the publication of this article.

REFERENCES

1. K. Naoi, K.I. Kawase and Y. Inoue, *J. Electrochem. Soc.*, **144**, L170 (1997); https://doi.org/10.1149/1.1837714
2. K. Naoi, M. Menda, H. Ooike and N. Oyama, *J. Electroanal. Chem. Interfacial Electrochem.*, **318**, 395 (1991); https://doi.org/10.1016/0022-0728(91)85321-F
3. N. Oyama, T. Tatsuma, T. Sato and T. Sotomura, *Nature*, **373**, 598 (1995); https://doi.org/10.1038/373598a0
4. D.M. De Leeuw, M.M.J. Simenon, A.R. Brown and R.E.F. Einerhand, *Synth. Met.*, **87**, 53 (1997); https://doi.org/10.1016/S0379-6779(97)80097-5
5. M. Josowicz, J. Janata and M. Levy, *J. Electrochem. Soc.*, **135**, 112 (1988); https://doi.org/10.1149/1.2095533
6. R.M. Cervino, W.E. Triaca and A.J. Arvia, *J. Electroanal. Chem. Interfacial Electrochem.*, **182**, 51 (1985); https://doi.org/10.1016/0368-1874(85)85439-3
7. W.A. Gazotti Jr., G. Casalbore-Miceli, S. Mitzakoff, A. Geri, M.C. Gallazzi and M.A. De Paoli, *Electrochim. Acta*, **44**, 1965 (1999); https://doi.org/10.1016/S0013-4686(98)00305-3
8. A. Ray, A.F. Richter, A.G. MacDiarmid and A.J. Epstein, *Synth. Met.*, **29**, 151 (1989); https://doi.org/10.1016/0379-6779(89)90290-7
9. G.E. Asturias, A.G. MacDiarmid, R.P. McCall and A.J. Epstein, *Synth. Met.*, **29**, 157 (1989); https://doi.org/10.1016/0379-6779(89)90291-9
10. S. Mu, *Synth. Met.*, **143**, 259 (2004); https://doi.org/10.1016/j.synthmet.2003.12.008
11. W.R. Salaneck, I. Lundström, W.S. Huang and A.G. MacDiarmid, *Synth. Met.*, **13**, 291 (1986); https://doi.org/10.1016/0379-6779(86)90190-6
12. R. Jamal, T. Abdiryim and I. Nurulla, *Polym. Adv. Technol.*, **19**, 1461 (2008); https://doi.org/10.1002/pat.1139
13. W.S. Huang, B.D. Humphrey and A.G. MacDiarmid, *J. Chem. Soc.*, **82**, 2385 (1986); https://doi.org/10.1039/F19868202385